

Light-Driven Expulsion of the Sterically Hinderer Ligand L in Tris-diimine Ruthenium(II) Complexes of the Ru(phen)₂(L)²⁺ Family: A Pronounced Ring Effect

Jean-Paul Collin,* Damien Jouvenot, Masatoshi Koizumi,[†] and Jean-Pierre Sauvage*

Laboratoire de Chimie Organo-Minérale, UMR 7513 du CNRS, Université Louis Pasteur, Faculté de Chimie, 4, rue Blaise Pascal, 67070 Strasbourg Cedex, France

Received February 17, 2005

Three new ruthenium(II) complexes have been prepared which contain two 1,10-phenanthroline units and a third sterically hinderer chelate. In one case, the hinderer ligand is a disubstituted 2,2'-bipyridine (bpy) attached to two very bulky manisyl groups. The two other systems are similar in terms of size of the hinderer groups (anisyl substituents) located close to the central metal. The complexes investigated in the Present Report are aimed at providing building blocks of future light-driven molecular machines. The photochemical expulsion of the sterically hinderer chelate has thus been studied by UV-vis spectroscopy and ¹H NMR. Surprisingly, the manisyl-containing complex turned out to be photochemically inert, indicating that a too bulky group acts as a protecting function versus decomplexation rather than as a destabilizing group. For the two other systems, a pronounced ring effect was observed: whereas the acyclic systems undergo fast photochemical expulsion of the bpy-based ligand, in the cyclic complex, the bpy-incorporating ring is decomplexed about 5 times less efficiently than the acyclic ligand of the previous case. These observations on the strong dependence of the photochemical behavior of the ruthenium(II) complexes on their structural properties are corroborated by X-ray diffraction studies on the three compounds investigated.

Introduction

Dynamic molecular systems in which a given part of the molecular system can be set in motion at will under the action of an external signal are often referred to as molecular machines or motors.¹ They are particularly promising in relation to nanomechanical devices and information storage and processing at the molecular level.² Among the many examples of such systems reported during the past decade, several examples of light-driven machines have been described.³ Most of them contain a photoisomerizable group such as an azo benzene derivative. The light impulse converts

the trans isomer to the cis isomer, leading to a significant change of the geometry of the photochemically active group and thus strongly modifying its ability to interact with a given part of the molecular system. As a consequence, a rearrangement may occur.⁴ Our group has proposed another approach of light-driven machines, on the basis of dissociative excited states. Complexes of the Ru(diimine)₃²⁺ family have been used extensively in light-induced electron- and energy-transfer processes,⁵ but photochemical ligand exchange has rather been considered a detrimental reaction till now. This process requires population of the ligand-field excited state from the triplet metal-to-ligand charge transfer (³MLCT) excited state. We have recently reported a few

* Authors to whom correspondence should be addressed. E-mail: sauvage@chimie.u-strasbg.fr (J.-P.S.); jpcollin@chimie.u-strasbg.fr (J.-P.C.).

[†] Present address: Graduate School of Pharmaceutical Sciences, The University of Tokyo, ERATO, Japan Science and Technology Agency (JST), Hongo, Bunkyo-ku, Tokyo 113-0033, Japan.

- (1) (a) Sauvage, J.-P. *Molecular Machines and Motors, Structure & Bonding*; Springer: Berlin, Heidelberg, 2001; Vol. 99. (b) Balzani, V.; Credi, A.; Raymo, F. M.; Stoddart, J. F. *Angew. Chem., Int. Ed.* **2000**, *39*, 3348–3391. (c) Kelly, T. R.; De Silva, H.; Silva, R. A. *Nature* **1999**, *401*, 150–152. (d) Collin, J. P.; Dietrich-Buchecker, C.; Gaviña, P.; Jimenez-Molero, M. C.; Sauvage, J.-P. *Acc. Chem. Res.* **2001**, *34*, 477–487. (e) Balzani, V.; Credi, A.; Venturi, M. *Pure Appl. Chem.* **2003**, *75*, 541–547.
- (2) (a) Feringa, B. L. *Molecular Switches*; Wiley-VCH: Weinheim, Germany, 2001. (b) Bissell, R. A.; Córdova, E.; Kaifer, A. E.; Stoddart, J. F. *Nature* **1994**, *369*, 133–137. (c) Fabbri, L.; Licchelli, M.; Pallavicini, P. *Acc. Chem. Res.* **1999**, *32*, 846–853.

- (3) (a) Ballardini, R.; Balzani, V.; Gandolfi, M. T.; Prodi, L.; Venturi, M.; Philp, D.; Ricketts, H. G.; Stoddart, J. F. *Angew. Chem., Int. Ed. Engl.* **1993**, *32*, 1301–1303. (b) (a) Livoreil, A.; Sauvage, J.-P.; Armaroli, N.; Balzani, V.; Flamigni, L.; Ventura, B. *J. Am. Chem. Soc.* **1997**, *119*, 12114–12124. (b) Armaroli, N.; Balzani, V.; Collin, J.-P.; Gaviña, P.; Sauvage, J.-P.; Ventura, B. *J. Am. Chem. Soc.* **1999**, *121*, 4397–4408. (c) Brouwer, A. M.; Frochot, C.; Gatti, F. G.; Leigh, D. A.; Mottier, L.; Paolucci, F.; Roffia, S.; Wurpel, G. W. H. *Science* **2001**, *291*, 2124–2128. (d) Leigh, D. A.; Wong, J. K. Y.; Dehez, F.; Zerbetto, F. *Nature* **2003**, *424*, 174–179.
- (4) (a) Murakami, H.; Kawabuchi, A.; Kotoo, K.; Kunitake, M.; Nakashima, N. *J. Am. Chem. Soc.* **1997**, *119*, 7605–7606. (b) Balzani, V.; Credi, A.; Marchioni, F.; Stoddart, J. F. *Chem. Commun.* **2001**, 1860–1861.

systems which demonstrate that this photochemical ligand substitution reaction can be utilized to induce molecular motion,⁶ including a ruthenium(II)-complexed pseudo-rotaxane⁷ and a related catenane.⁸ Unfortunately, because of poor geometrical control of the Ru(II) coordination sphere and of the use of a slightly too small ring, the pseudo-rotaxane was only prepared in low yield and with great difficulty: a large proportion of its nonthreaded isomer was formed which was exceedingly difficult to separate from the desired threaded complex. To avoid the isomerism problems encountered in the previous synthesis, we decided to use a 6,6'-diaryl-2,2'-bipyridine (dabipy) core, providing any ring constructed from this fragment with a very well defined cavity through which the axis of a future rotaxane should unambiguously be threaded after complexation of the metal center.

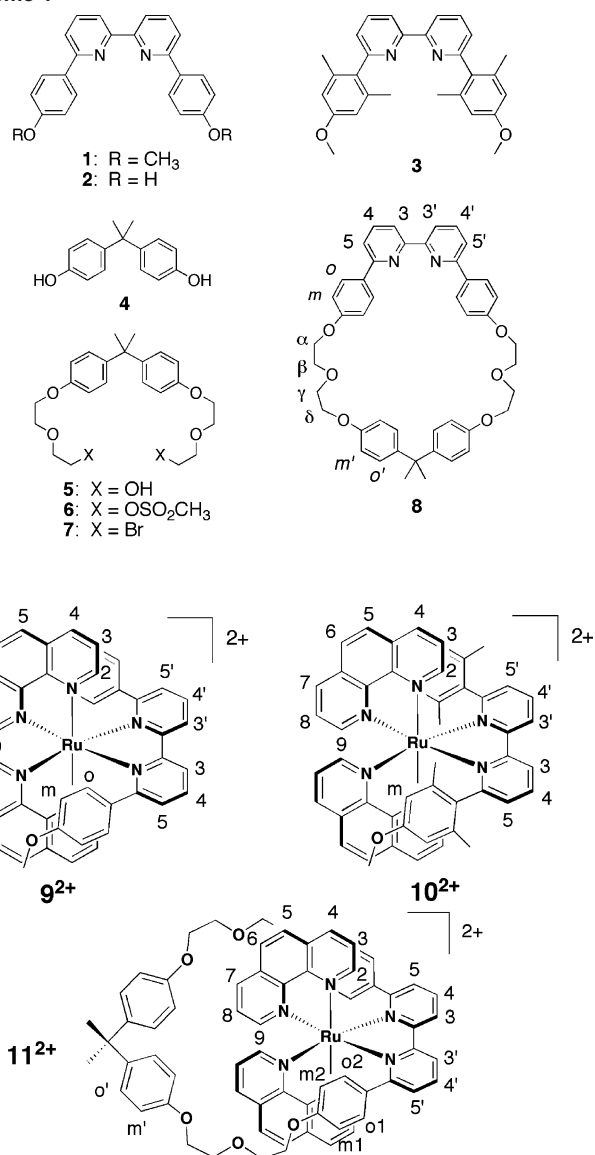
In the Present Report, we describe the synthesis of a dabipy-incorporating macrocycle (dabipy: 6,6'-diaryl-2,2'-bipyridine) and of its precursors as well as the corresponding ruthenium(II) complexes, the two additional chelates being phen nuclei (phen = 1,10-phenanthroline). X-ray studies demonstrate that the dabipy structure enforces the complexes to be "endo" complexes, that is, compounds in which the metal center is located in the internal site of the ring. Light-induced expulsion of the dabipy fragment takes place in a clean way by irradiating the compounds with white light, but a relatively strong ring effect was observed: when the dabipy fragment was incorporated in a 37-membered ring, the decoordination process was observed to be less efficient than in the analogous acyclic complex. By contrast, the photochemical expulsion is completely inhibited in a complex incorporating a bipyridine with two bulky manisyl groups. Another observation was made in relation to future light-driven machines regarding the size and nature of the substituents attached at the 6- and 6'-positions of the 2,2'-bipyridine chelate: the use of small substituents, such as methyl groups, seems to lead to much better quantum yields than that of larger aromatic groups.

Results and Discussion

Synthesis of the Ligands and Their Ruthenium(II) Complexes. The formula of the intermediates and of the target compounds are shown in Scheme 1.

6,6'-Di(4-anisyl)-2,2'-bipyridine (**1**) was synthesized in 76% yield by Suzuki coupling of 6,6'-dibromo-2,2'-bipyridine with 4-methoxyphenyl boronic acid in DME under reflux, in the presence of Pd[(C₆H₅)₃P]₄ and *tert*-C₄H₉OK

Scheme 1



as a base. Deprotection of the phenolic functions to give 6,6'-di(4-hydroxyphenyl)-2,2'-bipyridine (**2**) in quantitative yield was achieved with pyridine hydrochloride at 220 °C, according to a method previously described.⁹ The bipyridine ligand **3** was prepared following a modified procedure described previously.¹⁰ 4-Methoxy-2,6-dimethylphenyl boronic acid was used instead of the organozinc analogue. The 37-membered ring **8** containing a dimethyldi(4-alkoxyphenyl)methane fragment derived from bisphenol A (**4**) as well as a 6,6'-di(4-alkoxyphenyl)-2,2'-bipyridine unit can be obtained by macrocyclization between **3** and a suitable dibromo precursor, dimethyldi[4-(2-bromoethoxy)ethoxyphenyl]methane **7**, prepared from **4**. The diol **5** was obtained in 86% yield by reaction of **4** with 2-(2-iodoethoxy)ethanol in the presence of K₂CO₃ in DMF at 70 °C. The mesylation of **5** was achieved with methanesulfonyl chloride in the presence of triethylamine in CH₂Cl₂. Subsequent treatment of non-purified dimesylate **6** with LiBr in acetone gave **7** in 90%

- (5) (a) Meyer, T. J. *Acc. Chem. Res.* **1989**, *22*, 163–170. (b) Scandola, F.; Chiarboli, C.; Indelli, M. T.; Rampi, M. A. *Electron transfer in Chemistry*; Wiley-VCH: Weinheim, Germany, 2001; Vol. 3. (c) Sun, L.; Hammarström, L.; Akermark, B.; Styring, S. *Chem. Soc. Rev.* **2001**, *30*, 36–49. (d) Juris, A.; Balzani, V.; Barigelletti, F.; Campagna, S.; Belser, P.; Von Zelezvsky, A. *Coord. Chem. Rev.* **1988**, *84*, 85–277.
- (6) (a) Collin, J.-P.; Laemmel, A.-C.; Sauvage, J.-P. *New J. Chem.* **2001**, *25*, 22–24. (b) Schofield, E. R.; Collin, J.-P.; Gruber, N.; Sauvage, J.-P. *Chem. Commun.* **2003**, 188–189. (c) Baranoff, E.; Collin, J.-P.; Furusho, Y.; Laemmel, A.-C.; Sauvage, J.-P. *Chem. Commun.* **2000**, 1935–1936.
- (7) Pomeranc, D.; Jouvenot, D.; Chambron, J.-C.; Collin, J.-P.; Heitz, V.; Sauvage, J.-P. *Chem. Eur. J.* **2003**, *9*, 4247–4254.
- (8) Mobian, P.; Kern, J.-M.; Sauvage, J.-P. *Angew. Chem., Int. Ed.* **2004**, *43*, 2392–2395.

- (9) Curphey, T. J.; Hoffman, E. J.; McDonald, C. *Chem. Ind.* **1967**, 1138.
- (10) Loren, J. C.; Siegel, J. S. *Angew. Chem., Int. Ed.* **2001**, *40*, 754–757.

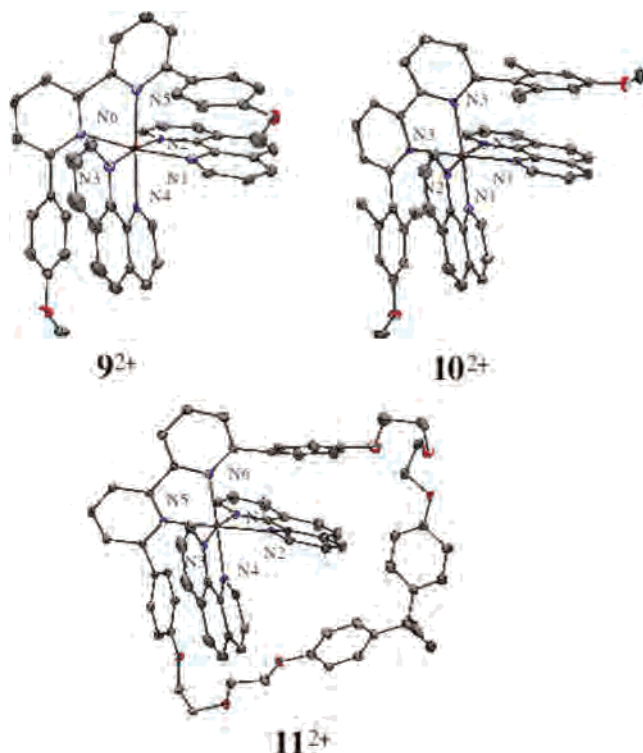


Figure 1. View of the crystal structures of the ruthenium complexes 9^{2+} , 10^{2+} , and 11^{2+} . Solvent molecules, H atoms, and anions are omitted for clarity. Ellipsoids are scaled to enclose 30% of the electronic density.

overall yield from **5**. The macrocycle **8** was synthesized in 32% yield by treating **2** with **7** under high dilution conditions, with Cs_2CO_3 as a base in DMF at 60 °C.

It was recently shown that $\text{cis-Ru}(\text{phen})_2(\text{CH}_3\text{CN})_2^{2+}$ was a more efficient starting material than the classical bis-chloro derivative $\text{cis-Ru}(\text{phen})_2\text{Cl}_2$ in order to introduce a third chelate on the ruthenium center.¹¹ Almost quantitative yields of $\text{Ru}(\text{phen})_2(\mathbf{1})(\text{PF}_6)_2$ [$9(\text{PF}_6)_2$] and $\text{Ru}(\text{phen})_2(\mathbf{8})(\text{PF}_6)_2$ [$11(\text{PF}_6)_2$] were obtained by heating a mixture of $\text{Ru}(\text{phen})_2(\text{CH}_3\text{CN})_2^{2+}$ and 1.5 equivalent of ligand (**1** or **8**) in ethylene glycol at 140 °C for 4 h. The crude products were purified by column chromatography after anion exchange by treatment with KPF_6 . By contrast, the same procedure applied to ligand **3** leads to the complex $\text{Ru}(\text{phen})_2(\mathbf{3})(\text{PF}_6)_2$ [$10(\text{PF}_6)_2$] in only 9% yield. This discrepancy can be ascribed to the large manisyl groups in close proximity of the coordinating nitrogen atoms.

Structural Properties of the Complexes. Suitable single crystals of compounds $9(\text{PF}_6)_2$, $10(\text{PF}_6)_2$, and $11(\text{PF}_6)_2$ were obtained by slow diffusion of an acetone solution of the complexes into toluene. The ORTEP diagrams of compounds 9^{2+} , 10^{2+} , and 11^{2+} with partial atomic numbering schemes are shown in Figure 1. Selected bond lengths and bond angles are given in Table 1.

In both structures, the N–Ru–N bond angles indicate that the geometry about the ruthenium atom is distorted from octahedral. As demonstrated in similar ruthenium complexes,^{11,12} this distortion mainly takes place in the plane of

Table 1. Selected Bond Lengths (Å) and Bond Angles (°) for $9(\text{PF}_6)_2$, $10(\text{PF}_6)_2$, and $10(\text{PF}_6)_2$

	$9(\text{PF}_6)_2$	$11(\text{PF}_6)_2$	$10(\text{PF}_6)_2$	
Ru N1	2.079(7)	2.078(4)	Ru N1	2.064(3)
Ru N2	2.073(8)	2.080(4)	Ru N1 ^a	2.064(3)
Ru N3	2.070(7)	2.051(4)	Ru N2	2.070(3)
Ru N4	2.074(7)	2.066(4)	Ru N2 ^a	2.070(3)
Ru N5	2.111(7)	2.099(4)	Ru N3	2.138(3)
Ru N6	2.116(7)	2.109(3)	Ru N3 ^a	2.138(3)
N1 Ru N2	79.2(3)	79.4(2)	N1 Ru N1 ^a	79.8(1)
N1 Ru N3	94.6(3)	172.1(1)	N1 Ru N2	79.6(1)
N1 Ru N4	80.2(3)	94.5(1)	N1 Ru N2 ^a	93.9(1)
N1 Ru N5	105.1(3)	93.4(2)	N1 Ru N3	173.7(1)
N1 Ru N6	175.9(3)	86.8(1)	N1 Ru N3 ^a	101.1(1)
N2 Ru N3	173.8(3)	94.1(2)	N1 ^a Ru N2	93.9(1)
N2 Ru N4	99.4(3)	78.8(1)	N1 ^a Ru N2 ^a	79.6(1)
N2 Ru N5	88.0(3)	172.7(2)	N1 ^a Ru N3	101.1(1)
N2 Ru N6	101.1(3)	101.2(1)	N1 ^a Ru N3 ^a	173.7(1)
N3 Ru N4	79.4(3)	79.7(1)	N2 Ru N2 ^a	171.5(1)
N3 Ru N5	93.6(3)	93.1(2)	N2 Ru N3	94.1(1)
N3 Ru N6	85.2(3)	98.9(1)	N2 Ru N3 ^a	92.4(1)
N4 Ru N5	171.7(3)	101.2(1)	N2 ^a Ru N3	92.4(1)
N4 Ru N6	95.7(3)	178.6(2)	N2 ^a Ru N3 ^a	94.1(1)
N5 Ru N6	79.1(3)	78.9(1)	N3 Ru N3 ^a	78.7(1)

^a Symmetry code: $-x + 1/2$; y ; $-z + 1/2$.

the bipyridine chelates and is due to the steric hindrance brought by the anisyl or manisyl groups. Thus, the two phenanthroline ligands are brought closer to one another, making the angle between the cis nitrogens of each ligand smaller than the expected 90° value. For the acyclic ligands, the distortion is also very strong on the bipyridine ligands (**1** and **3**) as indicated by the torsion angles N5–C–C–N6 and N3–C–C–N3 (19.6° and 26.2°, respectively, for 9^{2+} and 10^{2+}). Surprisingly, in the cyclic complex 11^{2+} , the torsion angle N5–C–C–N6 is only 0.74°. In this case, the ruthenium atom is outside the bipyridine plane and an unusual type of distortion, known as tilt displacement, is adopted.¹³ In both cases, the Ru–N bond lengths are larger for the bipyridine-type ligands than for the phenanthrolines (see Table 1). This clearly shows that the hindrance brought by the substituents in positions 6 and 6' of the bipyridine ligand induces a decrease of the ligand field, facilitating the expulsion of these ligands under visible light irradiation. However, the Ru–bipyridine lengths are larger in the case of the acyclic ligands than in the case of the cyclic one (where a tilt effect is observed). The macrocyclic chelate embraces the ruthenium bis-phenanthroline moiety and therefore keeps the latter closer to the ring. This behavior is confirmed by the X-ray analysis but can also be evidenced in solution using ¹H NMR spectroscopy. An efficient π -stacking can be observed between the anisyl and manisyl groups and the phenanthroline ligands. Because the two planes are not exactly parallel, the distances between the two planes are in the range of 2.76–3.38 Å for $9(\text{PF}_6)_2$, 3.08–3.48 Å for $10(\text{PF}_6)_2$, and 2.64–3.46 Å for $11(\text{PF}_6)_2$.

¹H NMR Spectroscopy. All the NMR resonances are sharp and well-resolved in the ¹H NMR spectrum of $10(\text{PF}_6)_2$ at room temperature. Since the sharp signals at 5.2 and 5.9 ppm can be assigned to the two protons in meta

(11) Baranoff, E.; Collin, J.-P.; Furusho, J.; Furusho, Y.; Laemmel, A.-C.; Sauvage, J.-P. *Inorg. Chem.* **2002**, *41*, 1215–1222.

(12) Ichida, H.; Tachiyashiki, S.; Sasaki, Y. *Chem. Lett.* **1989**, 1579–1580.
(13) Bonneson, P.; Walsh, J. I.; Pennington, W. T.; Cordes, A. W.; Durham, B. *Inorg. Chem.* **1983**, *22*, 1761–1765.

position of the two equivalent manisyl groups, the rotation of these very bulky substituents is completely suppressed. One of the most remarkable features in the ^1H NMR spectra of the complexes $\mathbf{9}(\text{PF}_6)_2$ and $\mathbf{11}(\text{PF}_6)_2$ is the splitting and the broadening of the peaks attributed to the anisyl groups. Because of the strong hindrance, the rotation of the anisyl groups is several orders of magnitude slower than for the free ligands. In the case of the free ligand, the protons of the anisyl groups display a set of two sharp doublets. On the other hand, once these ligands are coordinating the $[\text{Ru}(\text{phen})_2]$ fragment, the signals split into four broad peaks, as the symmetry is broken. The $[\text{Ru}(\text{phen})_2]$ fragment has a C_2 symmetry, and thus the two anisyl groups are equivalent. However, none of the protons of one anisyl are equivalent to the other, as this group is not allowed to rotate freely, at least at room temperature. This is why four peaks are observed. All the peaks could be attributed using 2D NMR techniques (COSY and ROESY). Remarkably, the chemical shift difference between the ortho protons is about 1.7 ppm. Indeed, o_1 is located in the shielding cone of the phenanthroline ligand, whereas o_2 is just above the ruthenium atom. The splitting is smaller for the meta protons as these are more distant from the metal center.

These spectra represent another evidence of the so-called ring effect. In the case of complex $\mathbf{9}^{2+}$, the signals are split and broad, but in the case of the macrocyclic complex $\mathbf{11}^{2+}$, this effect is more pronounced as we can even detect a coupling between adjacent protons (see Figure 2). This is an indication of a slower rotation. The rotational barriers were measured by recording ^1H NMR spectra at different temperatures (Figure 2). The spectra are recorded from 25 °C to 90 °C. At 65 °C, the coalescence of m_1 and m_2 was observed. At 90 °C, these two signals merge into a broad peak. We do not observe the same behavior for o_1 and o_2 since the chemical shift difference is too large to observe the merging of the peaks. The rotational barriers are of about $62.9 \text{ kJ}\cdot\text{mol}^{-1}$ for the acyclic complex $\mathbf{9}^{2+}$ and about $66.6 \text{ kJ}\cdot\text{mol}^{-1}$ for the macrocyclic one $\mathbf{11}^{2+}$. This difference of $3.7 \text{ kJ}\cdot\text{mol}^{-1}$ is more evidence of the fact that including a chelate in a macrocycle induces significant structural and dynamic changes compared to the acyclic analogue.

Photochemical Substitution Reactions. The photochemical expulsion of the bipyridine ligand and its substitution by two molecules of solvent (acetonitrile) can be followed either by UV–visible spectrometry or by ^1H NMR spectroscopy. The ^1H NMR experiment is done by irradiating (white light) a CD_3CN solution of the complex in an NMR tube. At the end of the irradiation, the ^1H NMR spectra correspond to the spectrum of $\text{Ru}(\text{phen})_2(\text{CD}_3\text{CN})_2^{2+}$ plus the fraction of ligand still soluble in CD_3CN (for complex $\mathbf{9}^{2+}$, the expelled ligand is completely insoluble in CD_3CN). Contrary to our expectation, the complex $\mathbf{10}^{2+}$ turned out photochemically very stable. No detectable evolution occurs after irradiation for 1 h by monitoring the reaction by UV–visible spectroscopy. A possible explanation of this behavior lies in the large size of the manisyl groups since no entering groups could reach the ruthenium atom after the photoinduced decoordination of the first pyridine subunit. In the case

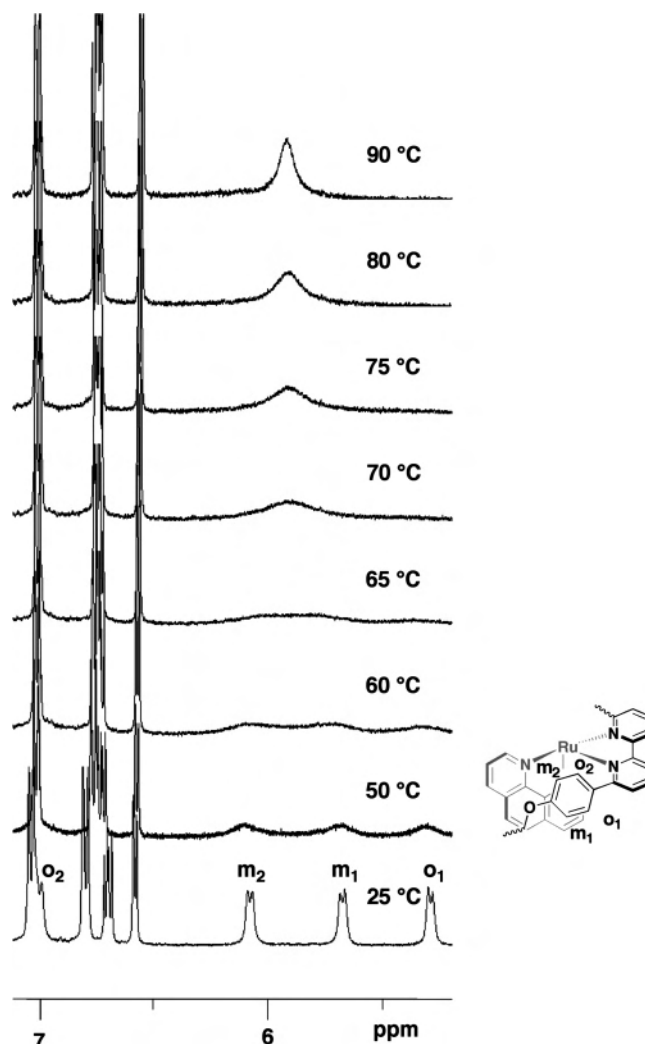


Figure 2. ^1H NMR spectra in CD_3SOCD_3 of the complex $\mathbf{11}^{2+}$ at different temperatures.

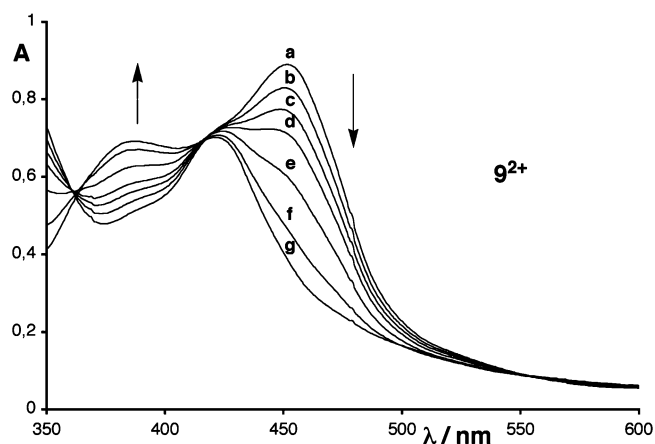


Figure 3. Electronic absorption spectra in CH_3CN of the complex $\mathbf{9}^{2+}$, before (a) and after different irradiation times (b: $t = 10 \text{ s}$; c: $t = 20 \text{ s}$; d: $t = 30 \text{ s}$; e: $t = 60 \text{ s}$; f: $t = 120 \text{ s}$; g: $t = 300 \text{ s}$).

of the complexes $\mathbf{9}^{2+}$ and $\mathbf{11}^{2+}$, hindering the bipyridine ligand at the 6 and 6' positions by smaller phenyl groups decreases the ligand field and allows a clean and quantitative expulsion of the bpy ligands $\mathbf{1}$ and $\mathbf{8}$, respectively. On Figure 3, the evolution of the absorption spectra of a degassed

acetonitrile solution of 9^{2+} is monitored as a function of the time of irradiation.

The final spectrum corresponds to the absorption spectrum of $\text{Ru}(\text{phen})_2(\text{CH}_3\text{CN})_2^{2+}$. For the two complexes 9^{2+} and 11^{2+} , the photochemical reactions proceed in a clean fashion: two isosbestic points are observed for each compound. Half-reaction times were calculated for both compounds under the same irradiation conditions. They correspond to 36 s for complex 9^{2+} and 173 s for complex 11^{2+} . This is more evidence of the macrocyclic effect that induces a remarkable rate difference in the photoexpulsion reaction. The macrocyclic ligand is expelled 5 times slower than the acyclic one. This result is consistent with the observations made on the crystal structure. As the Ru–N distances of the macrocyclic ligand are shorter than those of the acyclic one, the ligand field is higher in the macrocyclic complex and the population of the ^3MC state from the $^3\text{MLCT}$ excited state is less efficient. As a consequence, the expulsion of the ligand is significantly slowed. These processes are of great interest in the construction of light-driven molecular machines in which clean and efficient reactions are essential.

Experimental Section

General Methods. Oxygen- or moisture-sensitive reactions were performed in oven-dried glassware attached to a vacuum line with Schlenk techniques. Dry solvents were distilled from suitable desiccants under argon. Ligand **3** and $\text{Ru}(\text{phen})_2(\text{CH}_3\text{CN})_2(\text{PF}_6)_2$ were prepared according to literature procedures.^{10,14} All other chemicals were purchased from commercial sources and were used without further purification. Column chromatography was carried out on silica gel 60 [Merck, 40–63 (fine) or 63–200 mesh]. Thin-layer chromatography (TLC) was performed on glass plates coated with silica gel 60 F_{254} (Merck). ^1H NMR spectra were recorded with either Bruker AVANCE 300 (300 MHz) or Bruker AVANCE 400 (400 MHz) spectrometers with the deuterated solvent as the lock and residual solvent as the internal reference. The numbering schemes of the protons of the Ru-complexes and their precursors are indicated in Scheme 1. Fast atom bombardment mass spectra (FAB-MS) were recorded in positive-ion mode using 3-nitrobenzyl alcohol as a matrix with a ZAB-HF spectrometer. Electron spray ionization mass spectra (ESI-MS) were recorded with a Bruker MicroTOF instrument. UV/vis spectra (absorption spectroscopy) were recorded with a Kontron Instruments UVIKON 860 spectrometer at room temperature. All solutions were degassed and then saturated with oxygen-free argon. Light irradiation experiments: 3 mL of a sample solution of the complex ($C = 10^{-5}$ M) was put in a closed UV-visible glass cell. The sample was irradiated with the beam of a 250 W slide projector, filtered by a water filter, and focused on the cell. The use of a cutoff filter ($\lambda > 420$ nm) does not change significantly the course of the photochemical reactions. The evolution of the absorption spectrum of the solution was followed with respect to irradiation time. Single-crystal X-ray diffraction experiments were carried out using Kappa CCD and graphite-monochromated Mo $\text{K}\alpha$ radiation ($\lambda = 0.71073$ Å). For all computations, the MolEN package was used¹⁵ and structures were drawn using ORTEP.¹⁶ Crystal data and details of data collection for complexes **9**(PF_6)₂, **10**(PF_6)₂, and **11**(PF_6)₂ are provided in Table 2.

6,6'-Di(4-anisyl)-2,2'-bipyridine (1). 6,6'-Dibromopyridine (942 mg, 3.0 mmol), 4-methoxyphenylboronic acid (1.09 g, 7.2 mmol),

Table 2. Crystallographic Data of **9**(PF_6)₂, **10**(PF_6)₂, and **11**(PF_6)₂

	9(PF_6) ₂	10(PF_6) ₂	11(PF_6) ₂
formula	C103 H82 F24 N12 O5 P4 Ru2	C66 H60 F12 N6 O2 P2 Ru	C148 H134 F24 N12 O13 P4 Ru2
Mw	2349.88	1360.25	3070.79
cryst syst	monoclinic	monoclinic	triclinic
space group	C12/c1	P 1 2/n 1	P-1
<i>a</i> (Å)	29.1069(3)	11.5740(3)	13.8261(2)
<i>b</i> (Å)	16.7175(3)	14.6694(3)	15.1133(2)
<i>c</i> (Å)	24.5306(4)	17.7379(4)	17.0233(3)
α (deg)	90	90	102.063(5)
β (deg)	120.210(5)	95.684(5)	97.138(5)
γ (deg)	90	90	98.739(5)
<i>V</i> (Å ³)	10315.3(3)	2996.8(1)	3393.14(13)
<i>Z</i>	4	2	1
color	orange	orange	red
<i>D</i> _{calcd} (g cm ⁻³)	1.51	1.51	1.50
μ (mm ⁻¹)	0.457	0.404	0.371
<i>T</i> /K	173	173	173
<i>R</i> ^a	0.094	0.044	0.063
<i>R</i> _w ^b	0.118	0.058	0.084

$$^a R = \sum |F_o| - |F_c| / \sum |F_o|. \quad ^b R_w = [\sum w(|F_o| - |F_c|)^2 / \sum w(F_o^2)]^{1/2}.$$

and $\text{Pd}[\text{P}(\text{C}_6\text{H}_5)_3]_4$ (347 mg, 0.3 mmol) were placed in a two-necked round bottomed flask under argon. DME (15 mL) and 1.0 M *tert*-C₄H₉OK in *tert*-butyl alcohol (12 mL, 12.0 mmol), which had been degassed by bubbling, were added under a stream of argon. The mixture was degassed by three vacuum-filling with argon cycles and then was refluxed for 17 h. The solvents were evaporated to dryness and the residue was taken up in CH₂Cl₂/H₂O. The organic layer was dried with MgSO₄, and the solvents were evaporated to dryness. Acetone was added to the crude product to dissolve any byproducts and the white suspension was filtrated and washed with acetone to afford **1** (832 mg, 2.26 mmol) in 76% yield. ^1H NMR (300 MHz, 5% TFA/CD₂Cl₂, 25 °C): $\delta = 3.97$ (s, 6H, CH₃), 7.21 (d, 4H, *J* = 9.1 Hz, H_m), 8.05 (d, *J* = 9.1 Hz, H_o), 8.15 (dd, 2H, *J* = 1.5 and 7.6 Hz, H_{3,3'} or 5,5'), 8.35 (dd, 2H, *J* = 1.5 and 7.9 Hz, H_{5,5'} or 3,3'), 8.41 (dd, 2H, *J* = 7.6 and 7.9 Hz, H_{4,4'}) ppm. FAB-MS: *m/z* = 369.0 ([M + H]); calcd for C₂₄H₂₀N₂O₂ (M) 368.2.

6,6'-Di(4-hydroxyphenyl)-2,2'-bipyridine (2). Twelve molar hydrochloric acid (17 mL) was added to pyridine (16 mL) under argon with vigorous magnetic stirring. The flask was equipped for distillation and water was then distilled from the mixture until its internal temperature reached 220 °C. After cooling to 140 °C, **1** (830 mg, 2.25 mmol) was added as a solid and the reaction flask was then refluxed (215 °C) for 3 h under argon. The hot reaction mixture was diluted with hot water (10 mL) and was slowly poured into water (90 mL). The yellow suspension was then neutralized with a saturated KOH solution (monitored by pH-meter; endpoint: pH 7.2). After the neutralization, the suspension was filtrated, washed with water, and dried under high vacuum in the presence of P₂O₅ overnight to afford **2** (720 mg, 2.23 mmol) in 99% yield. ^1H NMR (300 MHz, CD₃OD, 25 °C): $\delta = 6.92$ (d, 2H, *J* = 8.8 Hz, H_m), 7.79 (dd, 2H, *J* = 1.0 and 7.9 Hz, H_{5,5'}), 7.91 (dd, 2H, *J* = 7.7 and 7.9 Hz, H_{4,4'}), 8.04 (d, 4H, *J* = 8.8 Hz, H_o), 8.40 (dd, 2H, *J* = 1.0 and 7.7 Hz, H_{3,3'}) ppm. FAB-MS: *m/z* = 341.1 ([M + H]); calcd for C₂₂H₁₆N₂O₂ (M) 340.1.

5. 4,4'-Isopropylidenediphenol (1.83 g, 8.0 mmol) and 2-(2-iodoethoxy)ethanol (5.18 g, 24.0 mmol) were added to a vigorously stirred suspension of K₂CO₃ (1.38 g, 10.0 mmol) in DMF (30 mL) under a stream of argon. The mixture was heated to 70 °C and

(14) Brown, G. M.; Callahan, R. W.; Meyer, T. J. *Inorg. Chem.* **1975**, *43*, 1915–1921.

(15) Fair, C. K. In *MolEN—An interactive intelligent system for crystal structure analysis*; Enraf-Nonius: Delft, The Netherlands, 1990.

(16) Johnson, C. K. *ORTEP-II: A FORTRAN Thermal Ellipsoid Plot Program for Crystal Structure Illustrations*; Report ORNL-5138; Oak Ridge National Laboratory: Oak Ridge, TN, 1976.

stirred for 20 h. DMF was removed in vacuo and the residue was taken up in diethyl ether/H₂O. The organic layer was washed with brine and H₂O and dried with MgSO₄, and the solvents were evaporated to dryness. The crude product was purified by column chromatography on silica gel (eluent: CH₂Cl₂/0–4% CH₃OH) affording pure **5** (2.77 g, 6.86 mmol) in 86% yield. ¹H NMR (300 MHz, CDCl₃, 25 °C): δ = 1.62 (s, 6H, (CH₃)₂), 3.64–3.68 (m, 4H, H_γ), 3.72–3.76 (m, 4H, H_β), 3.82–3.86 (m, 4H, H_δ), 4.09–4.12 (m, 4H, H_α), 6.81 (d, 4H, *J* = 8.9 Hz, H_{m'}), 7.12 (d, 4H, *J* = 8.9 Hz, H_{o'}) ppm. FAB-MS: *m/z* = 405.1 ([M + H]); calcd for C₂₃H₃₂O₆ (M) 404.2.

7. Methanesulfonyl chloride (852 mg, 4.5 mmol) in CH₂Cl₂ (10 mL) was added dropwise over 1 h to a solution of **5** (2.77 g, 6.86 mmol) and triethylamine (3.0 mL, 21.6 mmol) in CH₂Cl₂ (50 mL) at 0 °C. The solution was then stirred at 0 °C for 3 h, warmed to room temperature, and stirred for 15 h. H₂O was then added to the solution and it was stirred for an additional 1 h at room temperature. After decantation, the organic layer was washed with brine and H₂O and dried with MgSO₄, and the solvents were evaporated to dryness. The crude product of **6** (4.37 g) was used without further purification.

A solution of the crude product **6** (4.37 g) and LiBr (6.95 g, 80 mmol) in acetone (50 mL) was heated at reflux for 15 h. The solvent was then evaporated and the residue was taken up in CH₂Cl₂/H₂O. The organic layer was dried with MgSO₄, and the solvents were evaporated to dryness. The crude product was purified by column chromatography on silica gel (eluent: CH₂Cl₂/30–0% *n*-hexane) affording pure **7** (2.84 g, 5.36 mmol) in 78% yield. ¹H NMR (300 MHz, CDCl₃, 25 °C): δ = 1.65 (s, 6H, CH₃), 3.49 (t, 4H, *J* = 6.3 Hz, H_γ), 3.85–3.90 (m, 8H, H_α and H_β), 4.10–4.14 (m, 4H, H_δ), 6.83 (d, 4H, *J* = 8.9 Hz, H_{m'}), 7.14 (d, 4H, *J* = 8.9 Hz, H_{o'}) ppm. FAB-MS: *m/z* = 530.0 ([M⁺]); calcd for C₂₃H₃₀BrO₄ (M) 530.0.

8. A degassed mixture of **2** (681 mg, 2.0 mmol) and **7** (1.09 g, 2.06 mmol) in DMF (70 mL) was added dropwise over 100 h to a vigorously stirred suspension of Cs₂CO₃ (3.92 g, 12.0 mmol) in DMF (500 mL) at 60 °C under argon. After the addition, the mixture was stirred for an additional 12 h at 60 °C. DMF was removed in vacuo and the residue was taken up in CHCl₃ (ca. 500 mL). Silica (ca. 40 g) was added to the suspension and CHCl₃ was evaporated to dryness. The silica containing the crude product was charged on a silica gel column and was purified by chromatography (eluent: CH₂Cl₂/0–2% CH₃OH) followed by further column chromatography on fine silica gel (eluent: CH₂Cl₂/0–0.5% CH₃OH) affording pure **8** (459 mg, 0.648 mmol) in 32% yield. ¹H NMR (300 MHz, CDCl₃, 25 °C): δ = 1.60 (s, 6H, (CH₃)₂), 3.83–3.87 (m, 4H, H_γ), 3.91–3.95 (m, 4H, H_β), 4.03–4.07 (m, 4H, H_δ), 4.23–4.27 (m, 4H, H_α), 6.74 (d, 4H, *J* = 8.9 Hz, H_{m'}), 7.05 (d, 4H, *J* = 8.9 Hz, H_{o'}), 7.07 (d, 4H, *J* = 8.9 Hz, H_m), 7.73 (dd, 2H, *J* = 2.2 and 6.6 Hz, H_{3,3'}), 7.79–7.86 (m, 4H, H_{4,4'} and H_{5,5'}), 8.11 (d, 4H, *J* = 8.9 Hz, H_o) ppm. FAB-MS: *m/z* = 709.3 ([M + H]); calcd for C₄₅H₄₄N₂O₆ (M) 708.3.

Ru(phen)₂(1)(PF₆)₂ [9•(PF₆)₂]. A suspension of **1** (31.0 mg, 0.084 mmol) and Ru(phen)₂(CH₃CN)₂(PF₆)₂ (48.2 mg, 0.058 mmol) in degassed ethylene glycol (5 mL) was heated at 140 °C for 4 h under argon. The brown suspension turned dark-red solution. After cooling to room temperature, a saturated aqueous solution of KPF₆ (15 mL) was added. The orange precipitate was then filtrated and washed with water. The crude product was purified by column chromatography on silica gel [eluent: acetone/H₂O/saturated aqueous KNO₃ (100:0:0 to 100:8:0.8)] affording pure **9•(PF₆)₂** (64.2 mg, 0.057 mmol) in 99% yield. ¹H NMR (400 MHz, CD₃CN, 25 °C): δ = 3.58 (s, 6H, OCH₃), 5.34 (br s, 2H, H_o), 5.67 (br s, 2H, H_m), 6.18 (br s, 2H, H_m), 6.55 (dd, 2H, *J* = 1.3 and 5.4 Hz, H₂), 6.71 (dd, 2H, *J* = 5.4 and 8.1 Hz, H₃), 7.01 (br s, 2H, H_o), 7.68 (dd, 2H,

J = 1.4 and 7.8 Hz, H_{5,5'}), 7.94–8.00 (m, 6H, H_{4–5,8}), 8.09 (dd, 2H, *J* = 7.8 and 8.1 Hz, H_{4,4'}), 8.22 (d, 2H, *J* = 8.8 Hz, H₆), 8.64 (dd, 2H, *J* = 1.4 and 8.1 Hz, H_{3,3'}), 8.75 (dd, 2H, *J* = 1.2 and 8.3 Hz, H₉), 8.79 (dd, 2H, *J* = 1.2 and 5.2 Hz, H₇) ppm. ESI-MS: *m/z* = 975.16 ([M – PF₆]); calcd for C₄₈H₃₆F₆N₆O₂PRu = 975.15. The suitable single crystals of **9•(PF₆)₂** for X-ray analysis were obtained by a slow diffusion method at room temperature (toluene/acetone).

Ru(phen)₂(3)(PF₆)₂ [10•(PF₆)₂]. A suspension of **3** (20.0 mg, 0.042 mmol) and Ru(phen)₂(CH₃CN)₂(PF₆)₂ (35.0 mg, 0.042 mmol) in degassed ethylene glycol (5 mL) was heated at 140 °C for 2 h under argon. The brown suspension turned dark-red solution. After cooling to room temperature, a saturated aqueous solution of KPF₆ (15 mL) was added. The solution was extracted with ethyl acetate and the solvent was evaporated to dryness. The crude product was purified by column chromatography on silica gel [eluent: acetone/H₂O/saturated aqueous KNO₃ (100:0:0 to 100:5:0.5)] affording pure **10•(PF₆)₂** (4.7 mg, 0.0004 mmol) in 9% yield. ¹H NMR (300 MHz, (CD₃)₂CO, 25 °C): δ = 2.01 (s, 6H, CH₃), 2.11 (s, 6H, CH₃), 3.51 (s, 6H, OCH₃), 5.19 (d, 2H, *J* = 2.6 Hz, H_m), 5.90 (d, 2H, *J* = 2.6 Hz, H_m), 6.91 (dd, 2H, *J* = 5.3 and 8.1 Hz, H₃), 7.06 (dd, 2H, *J* = 1.3 and 5.3 Hz, H₂), 7.40 (dd, 2H, *J* = 1.4 and 7.7 Hz, H_{5,5'}), 8.13–8.18 (m, 6H, H_{4–5,8}), 8.42 (d, 2H, *J* = 8.9 Hz, H₆), 8.46 (dd, 2H, *J* = 7.7 and 8.1 Hz, H_{4,4'}), 8.80 (dd, 2H, *J* = 1.2 and 5.3 Hz, H₇) 8.96 (dd, 2H, *J* = 1.2 and 8.2 Hz, H₉), 9.12 (dd, 2H, *J* = 1.4 and 8.1 Hz, H_{3,3'}), ppm. ESI-MS: *m/z* = 1031.21 ([M – PF₆]); calcd for C₅₂H₄₄F₆N₆O₂PRu = 1031.22.

Ru(phen)₂(8)(PF₆)₂ [11•(PF₆)₂]. A suspension of **8** (14.2 mg, 0.02 mmol) and Ru(phen)₂(CH₃CN)₂(PF₆)₂ (16.7 mg, 0.02 mmol) in degassed ethylene glycol (3 mL) was heated at 140 °C for 2 h under argon. The brown suspension turned dark-red solution. After cooling to room temperature, a saturated aqueous solution of KPF₆ (10 mL) was added. The orange precipitate was then filtrated and washed with water. The crude product was purified by column chromatography on silica gel [eluent: acetone/H₂O/saturated aqueous KNO₃ (100:0:0 to 100:6:0.6)] affording pure **11•(PF₆)₂** (28.9 mg, 0.0198 mmol) in 99% yield. ¹H NMR (400 MHz, (CD₃)₂SO, 25 °C): δ = 1.57 (s, 6H, (CH₃)₂), 3.72–3.91 (br m, 12H, H_{α–γ}), 4.12–4.18 (br m, 4H, H_δ), 5.30 (br d, 2H, *J* = 7.8 Hz, H_o), 5.68 (br d, 2H, *J* = 7.8 Hz, H_m), 6.08 (br d, 2H, *J* = 7.8 Hz, H_m), 6.59 (dd, 2H, *J* = 0.8 and 5.4 Hz, H₂), 6.71 (dd, 2H, *J* = 5.4 and 8.0 Hz, H₃), 6.80 (d, 4H, *J* = 8.8 Hz, H_{m'}), 7.00 (br d, 2H, *J* = 7.8 Hz, H_o), 7.04 (d, 4H, *J* = 8.8 Hz, H_{o'}), 7.18 (dd, 2H, *J* = 1.0 and 7.6 Hz, H_{5,5'}), 7.96–8.03 (m, 6H, H_{4–5} and H₈), 8.14 (dd, 2H, *J* = 7.6 and 8.0 Hz, H_{4,4'}), 8.28 (d, 2H, *J* = 9.0 Hz, H₆), 8.83 (dd, 2H, *J* = 0.8 and 8.1 Hz, H₇), 8.84 (dd, 2H, *J* = 0.8 and 8.0 Hz, H_{3,3'}), 8.94 (dd, 2H, *J* = 0.8 and 5.2 Hz, H₉) ppm. ESI-MS: *m/z* = 1315.32 ([M – PF₆]); calcd for C₆₉H₆₀F₆N₆O₆PRu = 1315.32. The suitable single crystals of **11•(PF₆)₂** for X-ray analysis were obtained by a slow diffusion method at room temperature (toluene/acetone).

Acknowledgment. We would like to thank the CNRS and the French Ministry of Education, Research, and Technology for a fellowship (D.J.) for financial support. M.K. thanks the JSPS Postdoctoral Fellowship for Research Abroad. We thank André De Cian and Nathalie Gruber for the X-ray structures and also Johnson Matthey Inc. for a gift of RuCl₃.

Supporting Information Available: (S1) X-ray crystallographic files in cif format for the structure determination of compounds **9**²⁺, **10**²⁺, and **11**²⁺. This material is available free of charge via the Internet at <http://pubs.acs.org>.

IC050246A